Report on

Ambient Noise Measurements and Data Analyses in Duress city, Albania

Thessaloniki-Tirana, April 2020

Table of Contents

This Report is a joint effort of ITSAK-EPPO and IGEWE-PUT towards seismic risk reduction of the Durres city. The field-work, data processing & analyses and report preparation have been accomplished by the following researchers:

Institute of Engineering Seismology & Earthquake Engineering, ITSAK-EPPO, Thessaloniki, Greece
Theodoulidis Nikos
Grendas Ioannis

Institute of Geosciences, Energy, Water & Environment, IGEWE-PUT, Tirana, Albania
Duni Llambro
Dushi Edmond,
Kuka Neki
Koçi Rexhep
Bozo Rrezart
Gjuzi Olgert

1. Introduction

Despite the recent methodological and application developments, determining the seismic ground motion response of various geologic formations with traditional methods is still a difficult task. Such a task becomes even more difficult especially for large-scale urban areas that need to be densely covered, or in areas with moderate or low seismicity, due to the time period required to compile a statistically significant number of seismic records in order to acquire results based on traditional methods (for instance, Standard Spectral Ratio, SSR). Fortunately, in the last three decades ambient noise recordings have been extensively employed as a useful tool in determining local site effects due to seismic excitation. The most common technique, now almost routinely applied, relies on the calculation of the Horizontal to Vertical Spectral Ratio of ambient seismic noise, (Nakamura 1989, Bard 1999, 2004, Theodoulidis et al. 2004; among others).

After the disastrous earthquake of Nov. 26, 2019 in the vicinity of Durres city (Albania) it is of paramount importance to understand - among others - the role of geologic formation in seismic response. Basic soil dynamic properties (e.g. fundamental frequency, amplification, shear wave velocity) must be estimated for respective seismic response analysis. To this aim there are different approaches that could be applied each one with its plus and cons as well as various cost levels. There are two main categories of methods for in-situ site characterization; the actives and passive ones. The active ones (cross-hole, down-hole, CPT etc.) usually affect the environment and thus hardly can be implemented within cities. To the contrary, the passive methods are based on environmental mabient noise, they donot affect built environment and are much more cost effective in their application. One of the most popular and worldwide applied during the past few decades such method, is based on in-situ single-station ambient noise measurement and its proper data processing and analysis. The well known method uses the Horizontal-to-Vertical spectral ratio (HVSR) both of ambient noise (or microtremors) as well as of earthquake recordings at a site under investigation. This method can provide useful information regarding geologic layers fundamental frequency (fo), their corresponding amplitude (Ao) and

constrain shear wave velocity if it is used in joint inversion with dispersion curves (DC) calculated for a site. In addition, it is easily applied and of low-cost providing a first basicstep in microzonation studies.

The main target of the present work was to perform ambient noise measurements in the urban area of the Durres city (Albania) and apply the HVSR method on these measurements in an effort to calculate soil dynamic response parameters (e.g. fundamental and dominant frequency, their corresponding amplitudes). In addition, spatial distribution of these parameters is presented on maps of the city in order to be correlated with other available geological or/and geophysical properties of this geologically complex area. This is a preliminary work towards seismic microzonation of the Durres city. Additional geological, geophysical, geotechnical data would undoubtedly improve our understanding to seismic risk mitigation of the city and its suburbs.

2. Equipment and Measurements

For the single station ambient noise measurements two CitySharkII dataloggers (24-bits resolution) coupled with Lenartz-3D 5sec seismometers were used (Fig. 1,2). The response characteristics of Lenartz-3D 5sec are shown in Fig. 2.

Fig. 1. The CityShark datalogger used for ambient noise measurements in Durres city.

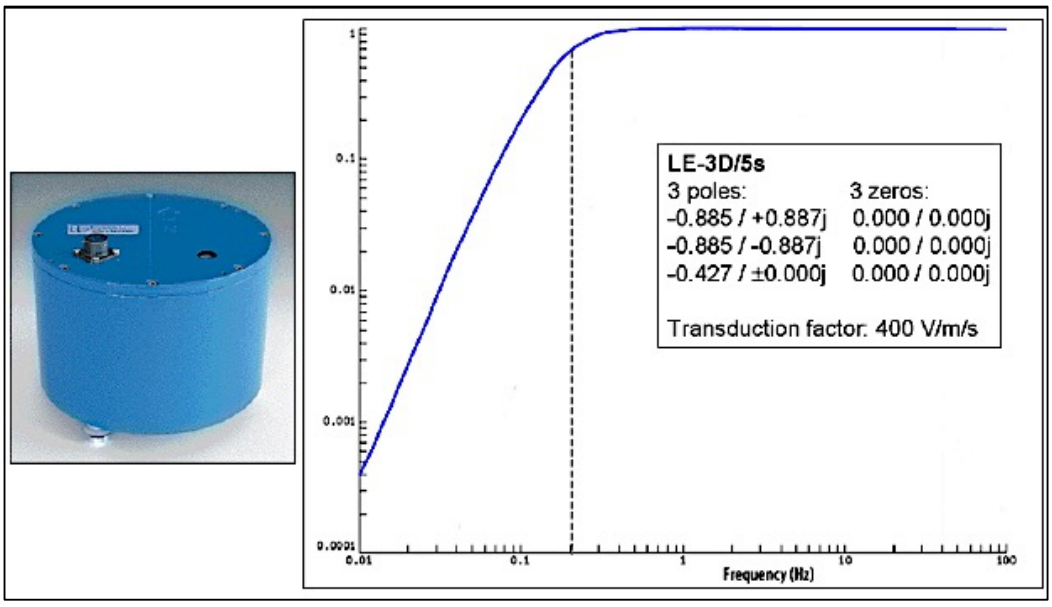

Fig. 2. The Lennartz-3D 5s seismometer used for ambient noise measurements in Durres city.

In the framework of the present work, 76 single-site measurements were performed in the city of Durres (Fig. 3, red dots) during the period 18 to 21 February, 2020. The majority of measurements was performed with a seismometer-to-ground coupling on soil conditions in order to avoid any high frequency 'contamination' from artificial surface layer (cement, asphalt, etc.). A typical ambient noise measurement installation is presented in Fig. 4. All measurements were acquired during the day, avoiding - as much as possible - the impact of near source manmade noise. The duration of measurement was 30min per site. The mesh of investigated sites was denser at the western part of the city, where higher structural damage was observed during the earthquake of Nov. 26, 2019. The respective field-work sheets are presented in Appendix 1 (Field Report on Ambient Noise Measurements).

The urbanization of the Durres city evolved on a soft sediment basin that is elongated in an almost north-south direction. A surface geology map (in scale 1:10.000) is shown in Fig. 5 (Kociu et al. 1985). Soft soil deposits of the Durres basin deepen from the edges to its center reaching a depth of ~130m (Fig. 6), indirectly implying low fundamental frequencies (fo<1Hz) for the majority of the investigated sites. Figures 5 and 6, were produced in the framework of an old microzonation study for the Durres city (Kociu et al. 1985). Information included in these Figures as well as any other relevant material of the old microzonation study will be useful to interpret results of the present work.

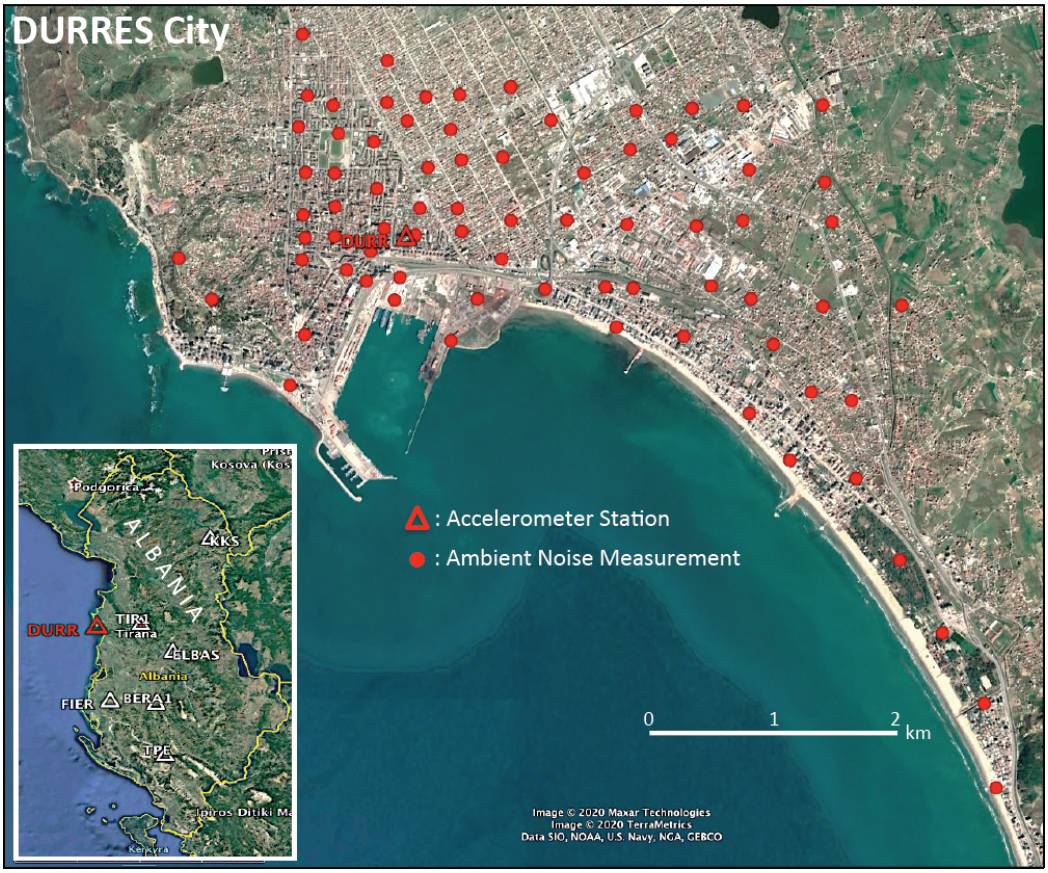

Fig. 3. Distribution of 76 sites where ambient noise measurements were performed.

Fig. 4. Typical ambient noise measurement installation (ground coupling) in Durres city.

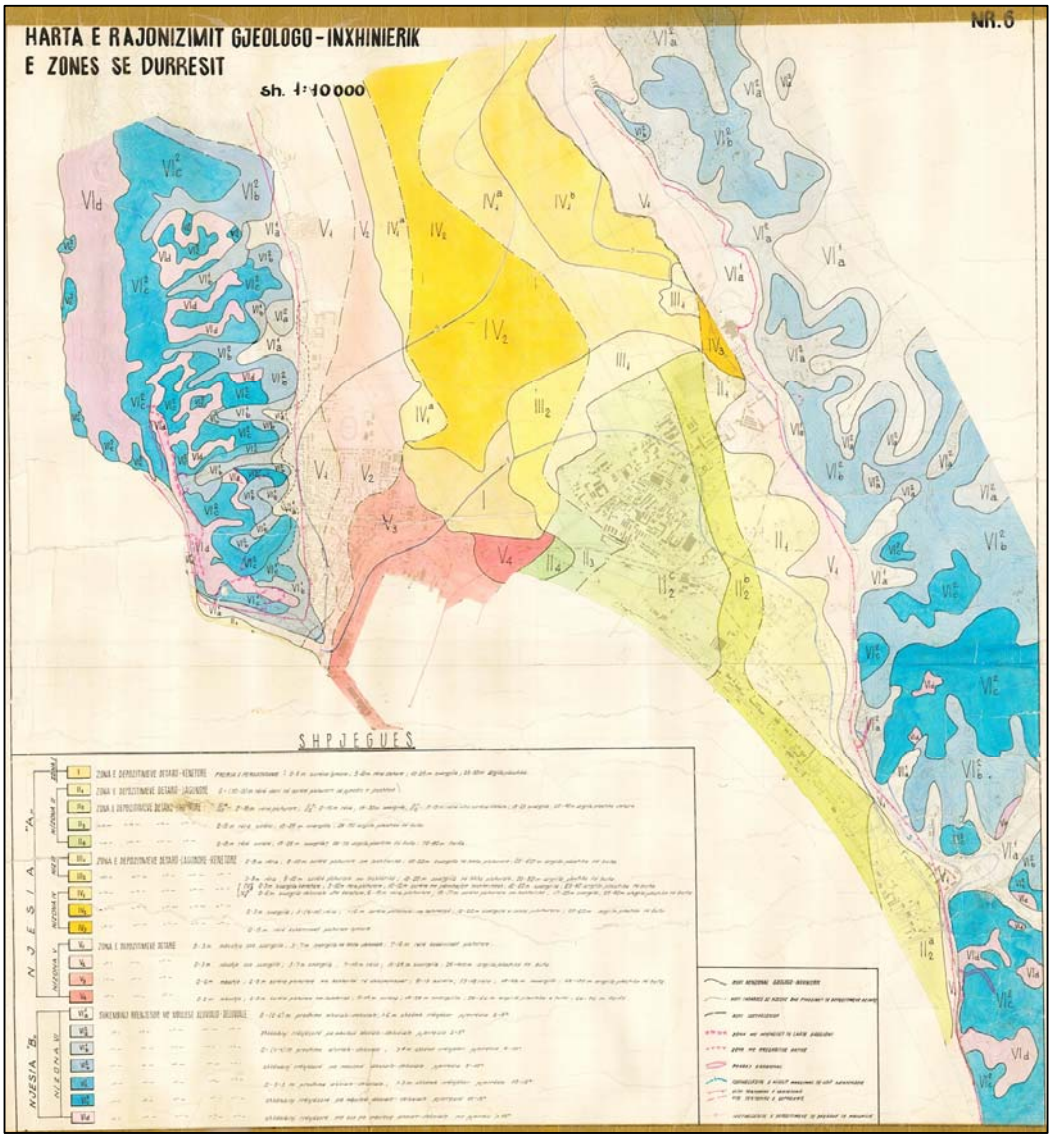

Fig. 5. Surface geology map of the Durres city and its suburbs (Microzonation of Durres city, scale 1:10.000, legend in Albanian, taken from Kociu et al. 1985).

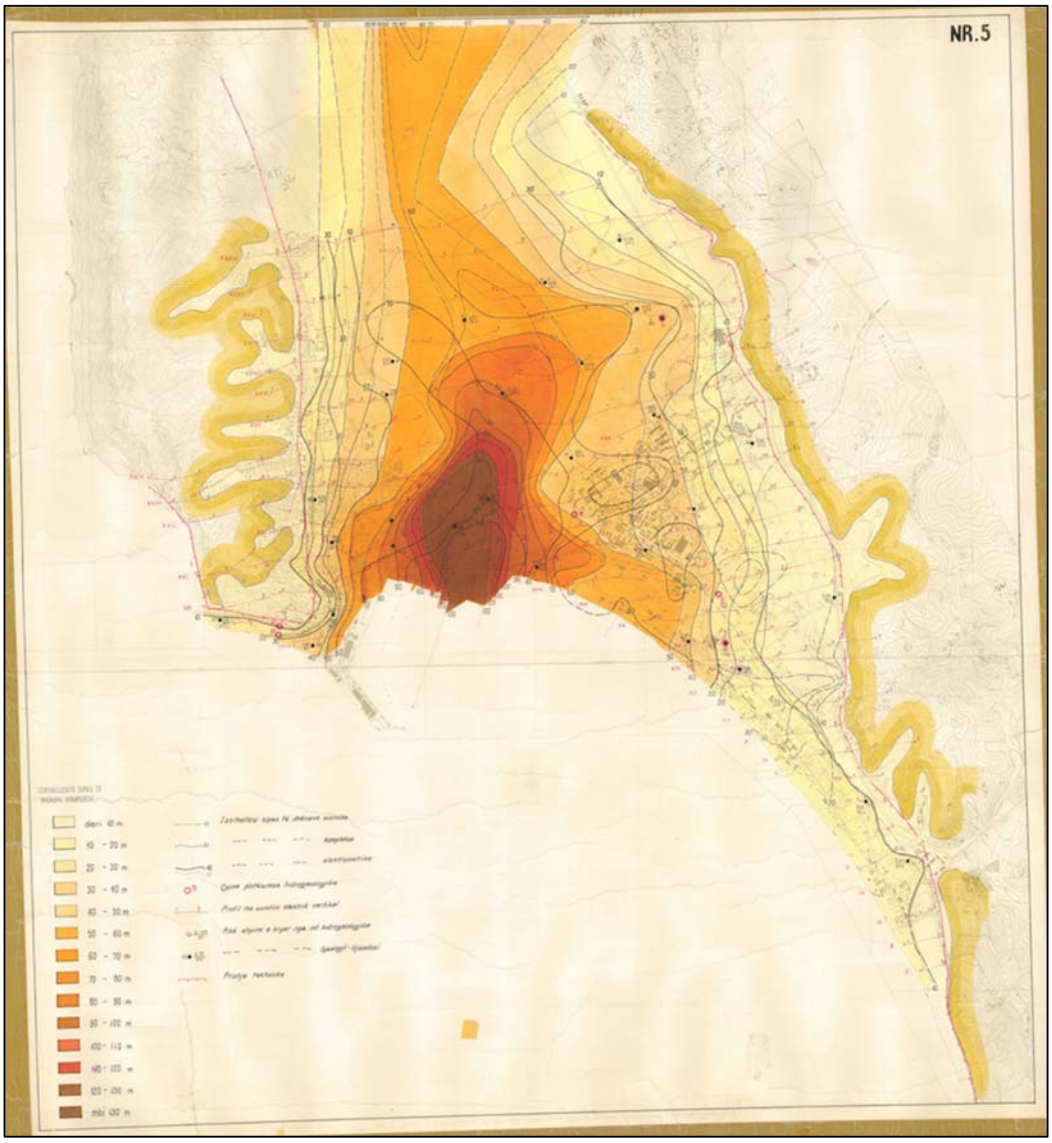

Fig. 6. Map with iso-depth contours for the Durres city up to geologic rock formation; the darkest the color the deepest the basin (Microzonation of Durres city, legend in Albanian, taken from Kociu et al. 1985).

3. Data Processing and Analyses

The data set was processed in a uniform way, using the Geopsy software package (www.geopsy.org). The complete ambient noise waveform was automatically divided in windows of 50sec each using the following parameters:

ShortTimeAverage=1sec, LongTimeAverage=30sec, min[STA/LTA]=0.20, max[STA/LTA]=2.5

Fourier transform was applied to each automatically selected window, with 5 % tapering and smoothed using the Konno and Ohmachi (1998) approach, with the b coefficient value set to 40. The mean horizontal spectra for each 50sec time window were derived by geometric averaging and the corresponding Horizontal-to-Vertical (H/V) spectral ratio was calculated. An example of the H/V processing using the 'geopsy' software (http://www.geopsy.org) is shown in Fig. 7. Certain criteria (see Fig. 8) to select H/V peaks as fundamental or higher mode frequency (ideal or/and clear peaks) were taken into account based on the SESAME guidelines (http://sesame.geopsy.org/SES_Reports.htm). For each site mean ±one standard deviation (H/V) spectral ratios were calculated and presented in Appendix 2: H/V Spectral Ratios for 76 Sites.

The H/V spectral ratio method was initially introduced by Nogoshi and Igarashi (1970) using single station ambient noise recordings to identify the resonance frequency of sediments formation overlain bedrock. Their idea was further developed by Nakamura (1989) and assumes that ambient noise is composed mainly of surface waves, with Rayleigh waves contributing to the vertical, while Love waves to the horizontal components. Consequently, a peak of the horizontal to vertical spectral ratio is considered to reveal the resonance frequency of the sediments overlain bedrock. Lachet and Bard (1994), Bard et al. (2004), Theodoulidis et al. (2004), confirmed this concept for simple one-dimensional structures. Although the resonance frequency potential of the method has been identified by various authors, its corresponding amplitude shows large variability. Haghshenas et al. (2008) proposed that the H/V spectral ratio peak amplitude provides a lower threshold of the amplification estimated from traditional methods, such as standard spectral

ratio (Borchertd 1970). To day it is widely accepted that the H/ spectral ratio amplitude - in general -is not directly related to local site amplification.

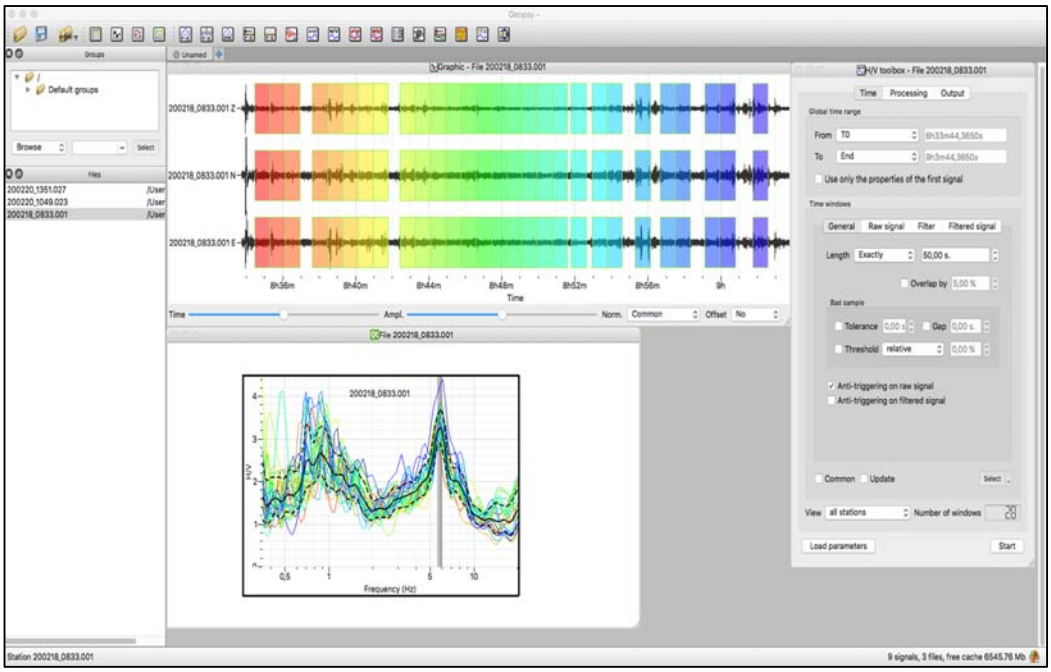

Fig. 7. Snapshot example of the H/V processing using the 'geopsy' software.

Criteria for a reliable H/V curve

i) $f_0 > 10 / l_w$

and

ii) $n_c(f_0) > 200$

and

iii) $\sigma_A(f)<2$ for $0.5f_0<f<2f_0$ if $f0>0.5Hz$

or $\sigma_A(f)<3$ for $0.5f_0<f<2f_0$ if $f0<0.5Hz$

Criteria for a clear H/V peak

(at least 5 out of 6 criteria fulfilled)

i) $\exists f^- \in [f_0/4, f_0] \mid A_{H/V}(f^-) < A_0/2$

ii) $\exists f^+ \in [f_0, 4f_0] \mid A_{H/V}(f^+) < A_0/2$

iii) $A_0 > 2$

iv) $f_{peak}[A_{H/V}(f) \pm \sigma_A(f)] = f_0 \pm 5\%$

v) $\sigma_f < \varepsilon(f_0)$

vi) $\sigma_A(f_0) < \theta(f_0)$

- l_w = window length
- n_w = number of windows selected for the average H/V curve
- $n_c = l_w \cdot n_w \cdot f_0$ = number of significant cycles
- f = current frequency
- f_{sensor} = sensor cut-off frequency
- f_0 = H/V peak frequency
- σ_f = standard deviation of H/V peak frequency ($f_0 \pm \sigma_f$)
- $\varepsilon(f_0)$ = threshold value for the stability condition $\sigma_f < \varepsilon(f_0)$
- A_0 = H/V peak amplitude at frequency f_0
- $A_{H/V}(f)$ = H/V curve amplitude at frequency f
- f^- = frequency between $f_0/4$ and f_0 for which $A_{H/V}(f^-) < A_0/2$
- f^+ = frequency between f_0 and $4f_0$ for which $A_{H/V}(f^+) < A_0/2$
- $\sigma_A(f)$ = "standard deviation" of $A_{H/V}(f)$, $\sigma_A(f)$ is the factor by which the mean $A_{H/V}(f)$ curve should be multiplied or divided
- $\sigma_{logH/V}(f)$ = standard deviation of the $\log A_{H/V}(f)$ curve, $\sigma_{logH/V}(f)$ is an absolute value which should be added to or subtracted from the mean $\log A_{H/V}(f)$ curve
- $\theta(f_0)$ = threshold value for the stability condition $\sigma_A(f) < \theta(f_0)$
- $V_{s,av}$ = average S-wave velocity of the total deposits
- $V_{s,surf}$ = S-wave velocity of the surface layer
- h = depth to bedrock
- h_{min} = lower-bound estimate of h

Threshold Values for σ_f and $\sigma_A(f_0)$

Frequency range [Hz]	< 0.2	0.2 – 0.5	0.5 – 1.0	1.0 – 2.0	> 2.0
$\varepsilon(f_0)$ [Hz]	0.25 f_0	0.20 f_0	0.15 f_0	0.10 f_0	0.05 f_0
$\theta(f_0)$ for $\sigma_A(f_0)$	3.0	2.5	2.0	1.78	1.58
$\log\theta(f_0)$ for $\sigma_{logH/V}(f_0)$	0.48	0.40	0.30	0.25	0.20

Fig. 8. Criteria for reliability of H/V results based on ambient noise measurements.

4. Results

Based on the average H/V spectral ratios for the 76 examined sites in the Durres city, as well as on the SESAME guidelines (http://sesame.geopsy.org/SES_Reports.htm), the following parameters were extracted, calculated and plotted on the map to study their spatial variability:

- The fundamental frequency, fo, and its corresponding amplitude, Ao.
- The dominant frequency, fd, and its corresponding amplitude, Ad. For the majority of sites fo equals to fd. However, in cases where the amplitude of the H/V spectral ratio for a certain frequency, f (with f>fo) was higher than that of the fundamental frequency corresponding amplitude, it was selected as dominant frequency, fd.
- The 'second peak' natural frequency, f1, and its coresponding amplitude, A1. Theoretical and numerical investigations have shown that such a situation occurs for two large impedance contrasts at two different scales: one for a thick structure and the other one for a shallower one. The two frequencies, f0 and f1 (with f0 < f1), may then be interpreted as characteristics at each scale, f0 being the fundamental frequency.
- The ground vulnerability index, $kg=(Ao)^2/fo$, as proposed by Nakamura (2000). The kg value is considered as an estimator, related to expected earthquake damage.

In Figures 9 and 10, fundamental frequencies, fo, and their corresponding amplitudes, Ao, are plotted on the urban area of Durres. Values of fo are grouped in three categories; [0.3Hz≤fo<1Hz], [1≤fo<2Hz], [2Hz≤fo≤5Hz]. A site with a flat H/V spectral ratio (Ao<2) is also presented, as with fo=20Hz. The majority of examined sites (84%) exhibit a fundamental frequency lower than 2Hz. Values of Ao are grouped in three categories; [Ao≥3.0], [2<Ao<3], [Ao≤2]. The vast majority of examined sites (95%) exhibit an amplitude greater than 2. In these Figures, as a background layer, the isodepth contours per 10m with a maximum depth of 130m in the center of the basin, are also shown.

In Figures 11 and 12, dominant frequencies, fd, and their corresponding amplitudes, Ad, are plotted on the urban area of Durres. Values of fd are grouped in three categories; [0.3Hz≤fd<1Hz], [1≤fd<2Hz], [2Hz≤fd≤5.9Hz]. A site with a flat H/V spectral ratio (Ao<2) is also presented as with fo=20Hz. The majority of examined sites (81%) exhibit a dominant frequency lower than 2Hz. Values of Ad are grouped in three categories; [Ad≥3.0], [2<Ad<3], [Ad≤2]. The vast majority of examined sites (95%) exhibit an amplitude greater than 2. In these Figures, as a background layer, the isodepth contours per 10m with a maximum depth of 130m in the center of the basin, are also shown.

In Figures 13 and 14, the sites showing a second peak of natural frequency, f1, (with f1>fo) and their corresponding amplitudes A1, are shown. These fifteen (15) sites are restricted at edges of the basin, mainly at its western side. Values of f1 are grouped in two categories; [f1≤1Hz], [f1>1Hz]. Values of A1 are also grouped in two categories; [A1≥3.0], [2≤A1<3]. In these Figures, as a background layer, the isodepth contours per 10m with a maximum depth of 130m in the center of the basin, are also shown.

A quantitative presentation of the map of Figure 9 is presented in Fig. 15, exhibiting satisfactory correlation between the thickness of sediments and fundamental frequency in the study area. However, the dispersion of fundamental frequency as a function of depth, H, for H>20m is smaller than those for H<20 m, in higher frequency range. Such a dispersion may be due to more superficial strata properties (e.g. soft colluvium, man-made deposits). Further geophysical and geotechnical investigation is necessary to lighten this issue.

In Figures 16, 17, 18, 19, 20, 21, values of fo, Ao, f1, A1, fd, Ad, are plotted on the urban area of Durres, as is made in Figures 9, 10, 11, 12, 13, 14, respectively, but with background layer that of surface geology (see Fig. 5).

In Figure 22, values of ground vulnerability index, Kgo, with respect to fundamental frequency fo and its corresponding amplitude Ao, are plotted on the urban area of Durres. Values of Kgo are grouped in four categories; [20≤Kgo≤95], [10≤Kgo<20], [1≤Kgo<10], [Kgo<1]. The majority of examined sites (62%) exhibit a ground vulnerability index greater than 10.

Similarly, in Figure 23 values of ground vulnerability index, Kgd, with respect to dominant frequency fd and its corresponding amplitude Ad, are also shown. In fact, both approaches, using either Kgo or Kgd, give almost identical results. In Figures 22 and 23, as a background layer, the isodepth contours per 10m with a maximum depth of 130m in the center of the basin, are also shown.

Finally, in Figures 24 and 25, values of Kgo and Kgd, are plotted on the urban area of Durres, as is made in Figures 22 and 23, respectively, but with background layer that of surface geology (see Fig. 5).

Fig. 9. Distribution of fundamental frequency, fo, in the Durres city. For sites in areas with red dashed line [0.3Hz≤fo<1Hz], with orange dashed line [1≤fo<2Hz] and with yellow dashed line [2Hz≤fo≤5Hz], are included. In blue dashed line a site with flat HVSR is included. Background layer isodepth contours per 10m (see Fig. 6).

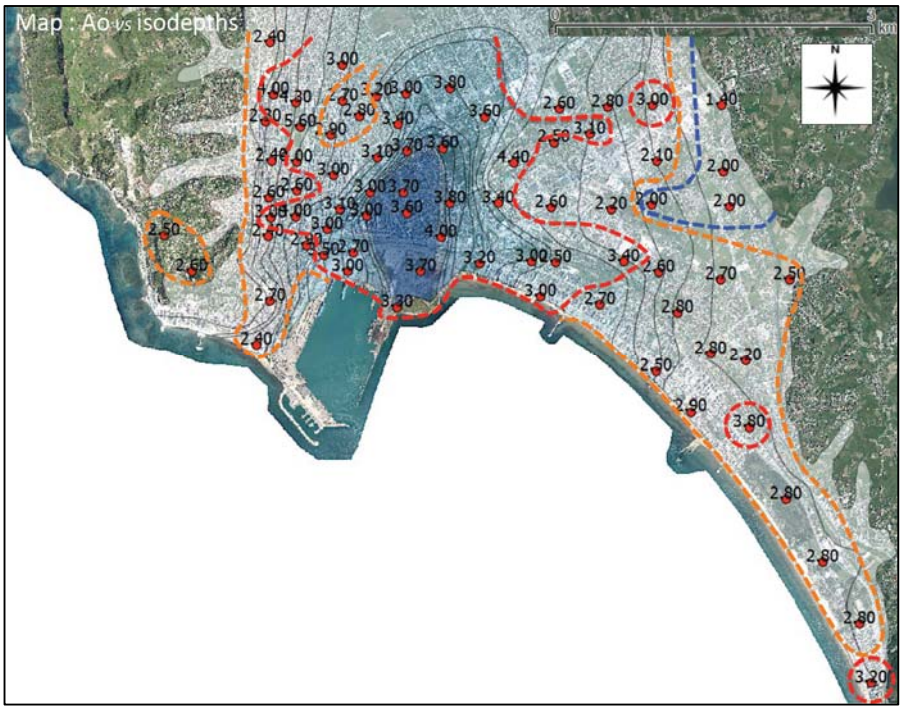

Fig. 10. Distribution of fundamental frequency corresponding amplitude, Ao, in the Durres city. For sites in areas with red dashed line [Ao≥3.0], with orange dashed line [2<Ao<3] and with blue dashed line [Ao≤2], are included. Background layer isodepth contours per 10m. Background layer isodepth contours per 10m(see Fig. 6).

Fig. 11. Distribution of dominant frequency, fd, in the Durres city. For sites in areas with red dashed line [0.3Hz≤fd<1Hz], with orange dashed line [1≤fd<2Hz] and with yellow dashed line [0.3Hz≤fd≤5Hz], are included. In blue dashed line a site with flat HVSR is included. Background layer isodepth contours per 10m(see Fig. 6).

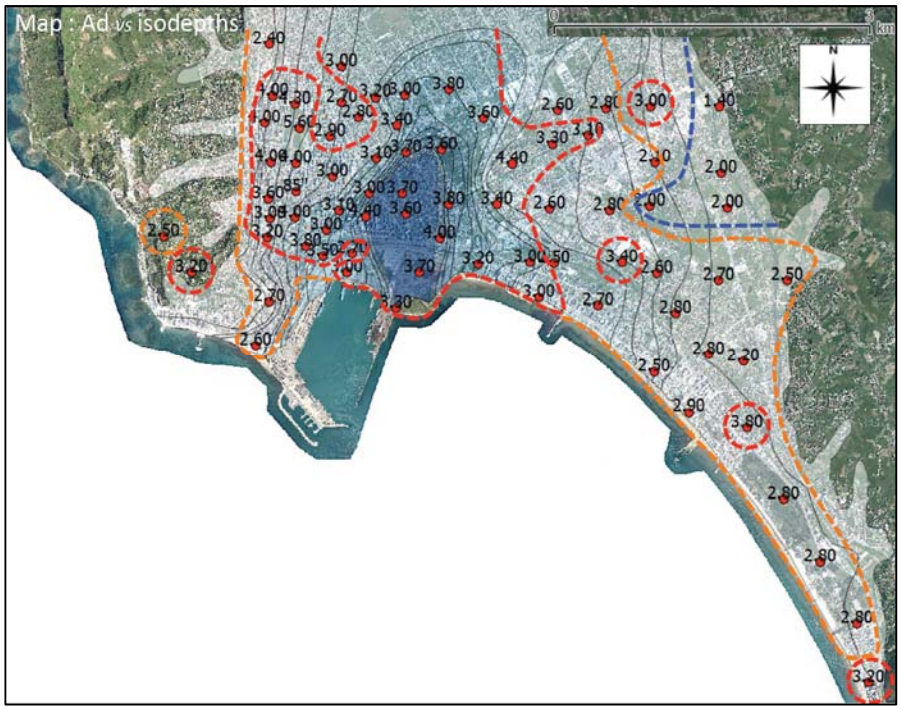

Fig. 12. Distribution of dominant frequency corresponding amplitude, Ad, in the Durres city. For sites in areas with red dashed line [Ad≥3.0], with orange dashed line [2<Ad<3] and with blue dashed line [Ad≤2], are included. Background layer isodepth contours per 10m(see Fig. 6).

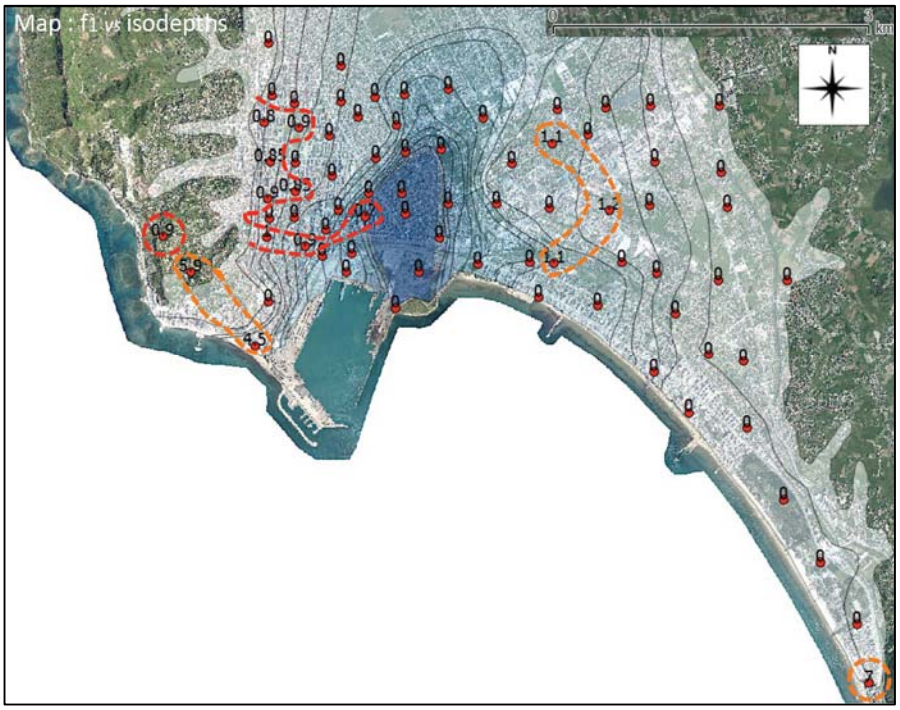

Fig. 13. Distribution of a second peak natural frequency, f_1, in the Durres city. For sites in areas with red dashed line [$f_1 \leq 1$Hz] and with orange dashed line [$f_1 > 1$Hz], are included. Background layer isodepth contours per 10m(see Fig. 6).

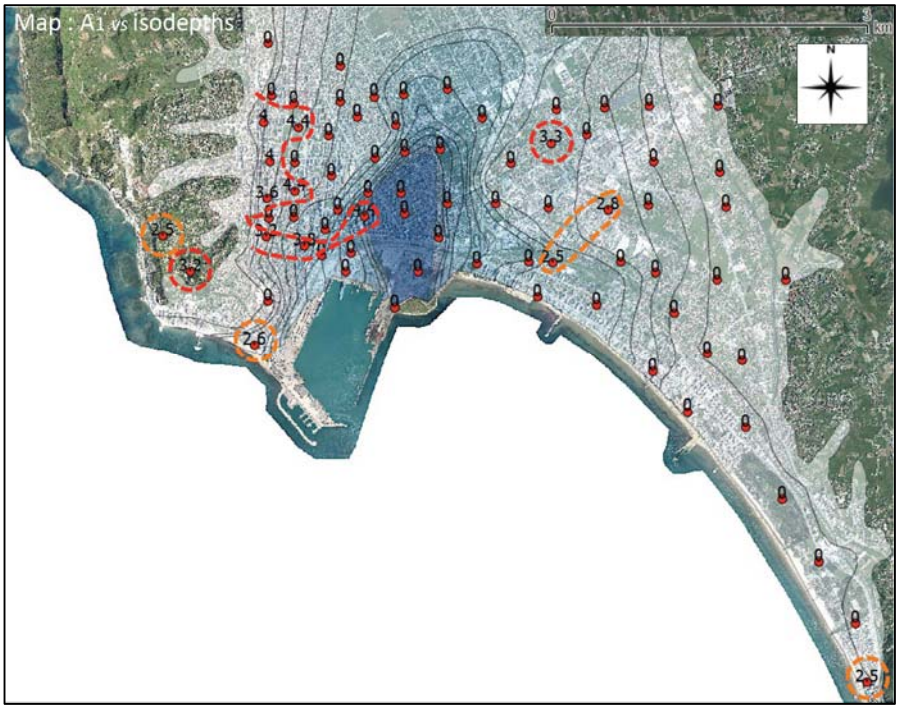

Fig. 14. Distribution of a second peak natural frequency corresponding amplitude, A_1, in the Durres city. For sites in areas with red dashed line [$A_1 \geq 3$] and with orange dashed line [$2 \leq A_1 < 3$], are included. Background layer isodepth contours per 10m(see Fig. 6).

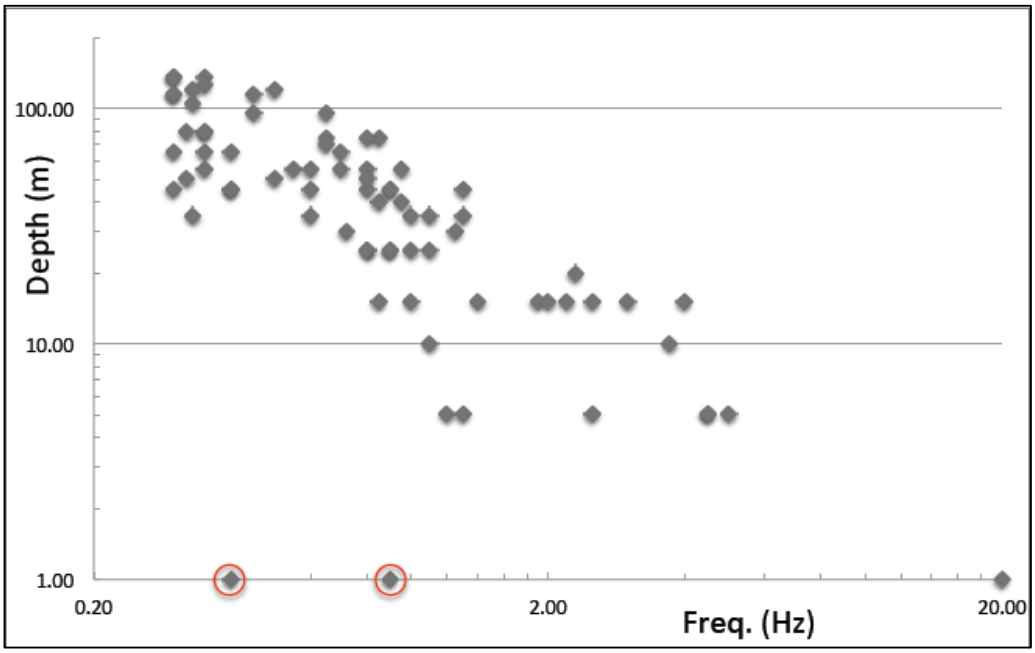

Fig. 15. Variation of fundamental frequency (fo) with depth in the Durres city. In red circles deviated points as outliers.

Fig. 16. Distribution of fundamental frequency, fo, in the Durres city. For sites in areas with red dashed line [0.3Hz≤fo<1Hz], with orange dashed line [1≤fo<2Hz] and with yellow dashed line [0.3Hz≤fo≤5Hz], are included. In blue dashed line a site with flat HVSR is included. Background layer surface geology (see Fig. 5).

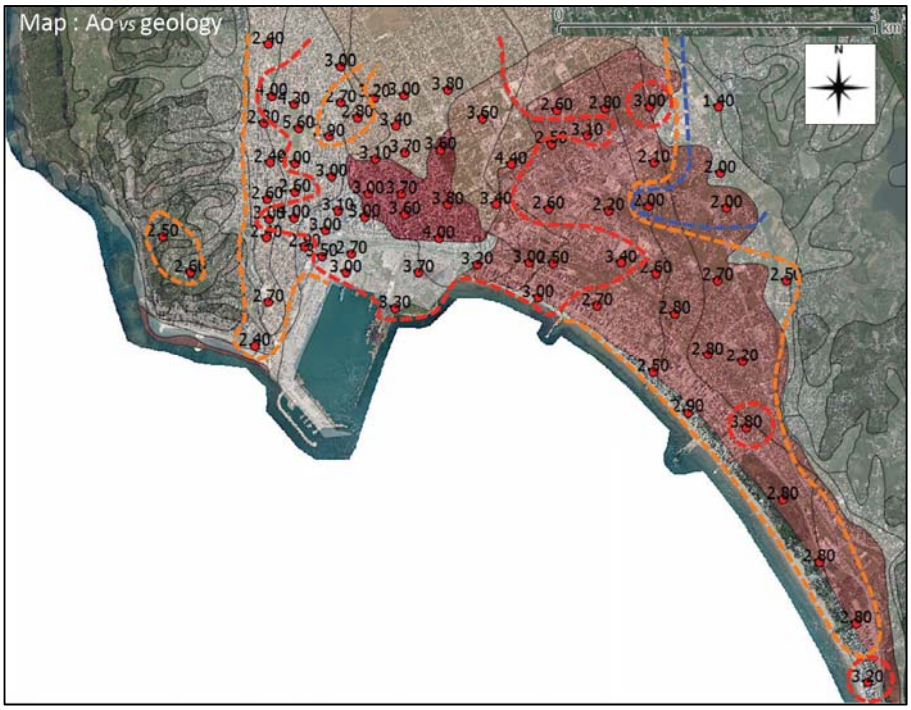

Fig. 17. Distribution of fundamental frequency corresponding amplitude, Ao, in the Durres city. For sites in areas with red dashed line [Ao≥3.0], with orange dashed line [2<Ao<3] and with blue dashed line [Ao≤2], are included. Background layer isodepth contours per 10m. Background layer surface geology (see Fig. 5).

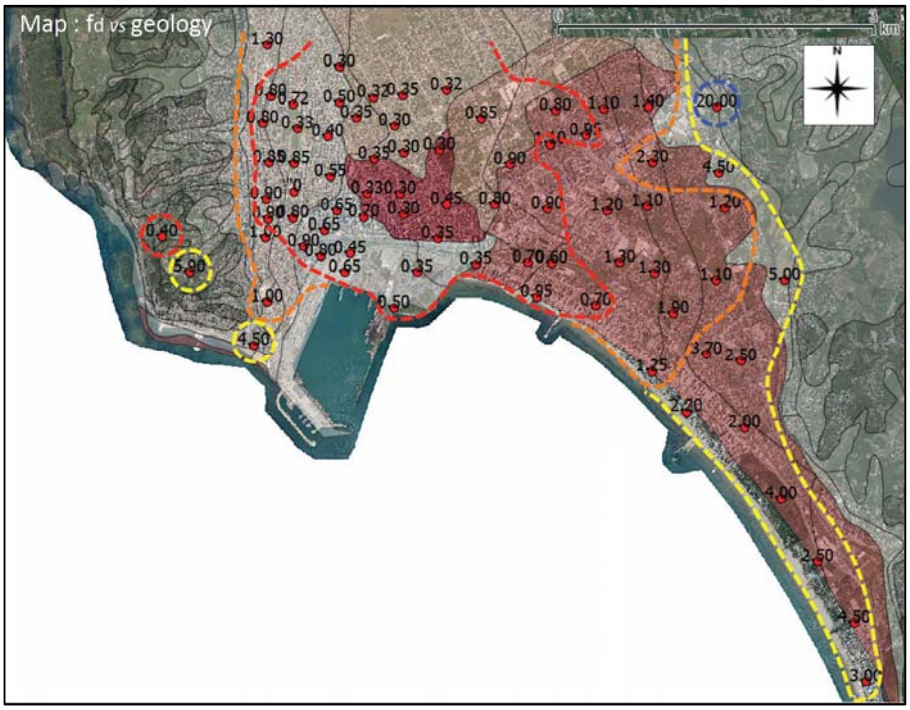

Fig. 18. Distribution of dominant frequency, fd, in the Durres city. For sites in areas with red dashed line [0.3Hz≤fd<1Hz], with orange dashed line [1≤fd<2Hz] and with yellow dashed line [0.3Hz≤fd≤5Hz], are included. In blue dashed line a site with flat HVSR is included. Background layer surface geology (see Fig. 5).

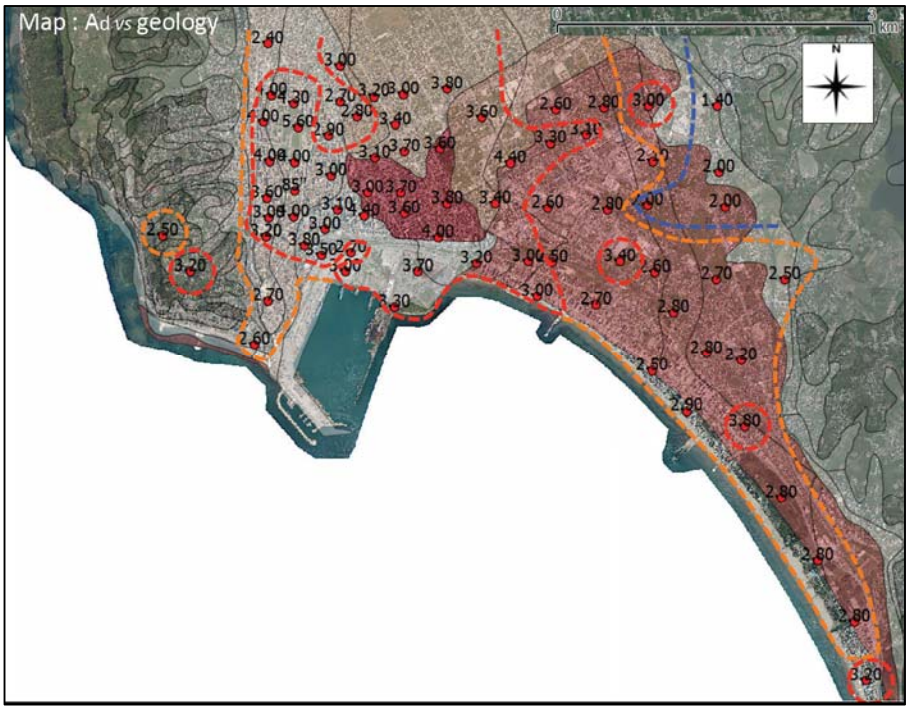

Fig. 19. Distribution of dominant frequency corresponding amplitude, Ad, in the Durres city. For sites in areas with red dashed line [Ad≥3.0], with orange dashed line [2<Ad<3] and with blue dashed line [Ad≤2], are included. Background layer surface geology (see Fig. 5).

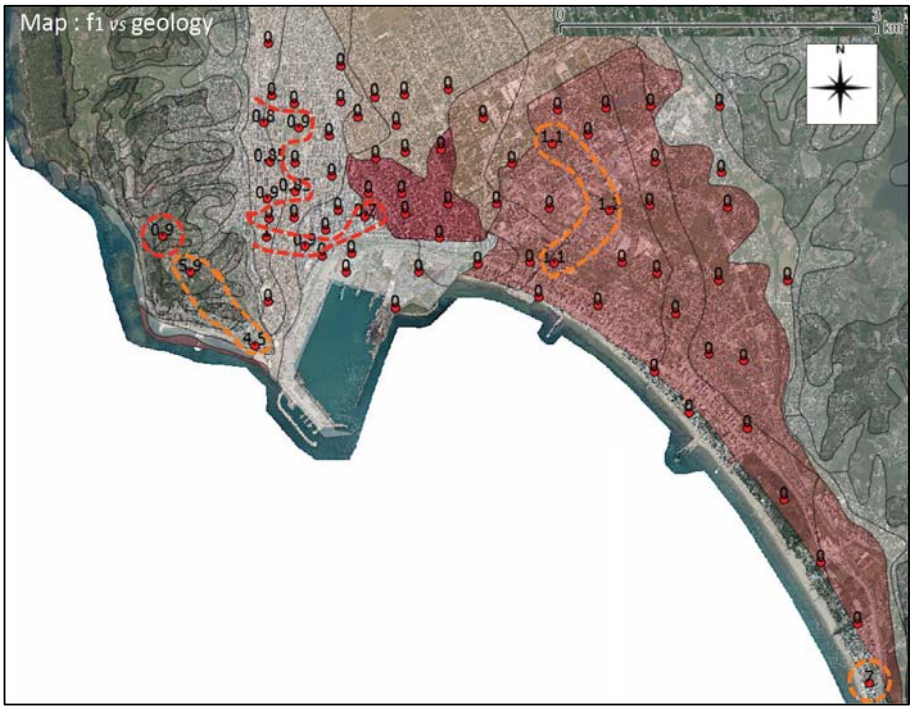

Fig. 20. Distribution of a second peak natural frequency, f_1, in the Durres city. For sites in areas with red dashed line [$f_1 \leq 1$Hz] and with orange dashed line [$f_1 > 1$Hz], are included. Background layer surface geology (see Fig. 5).

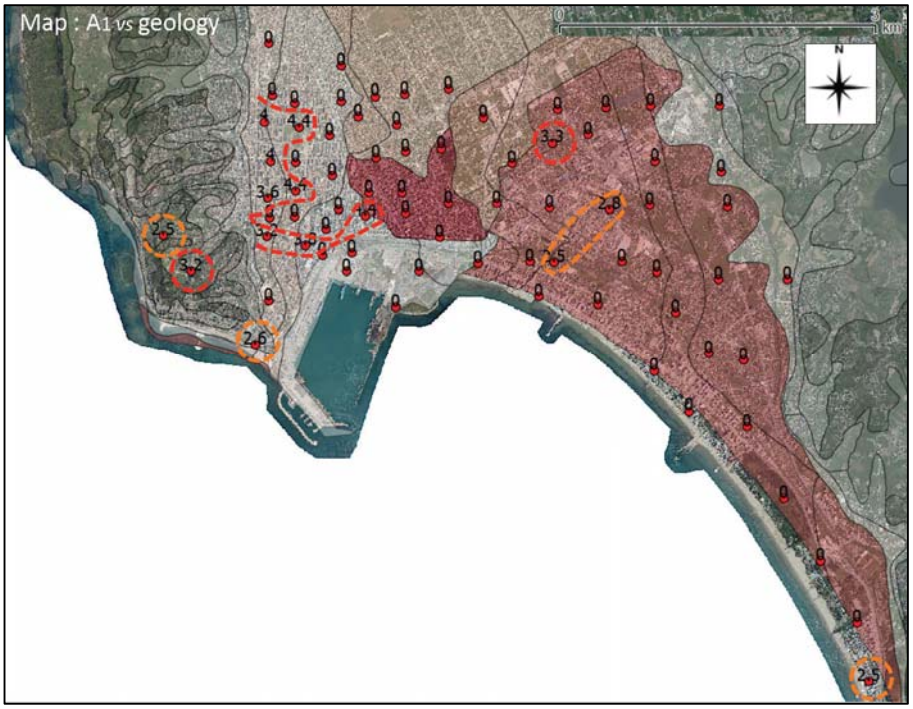

Fig. 21. Distribution of a second peak natural frequency corresponding amplitude, A_1, in the Durres city. For sites in areas with red dashed line [$A_1 \geq 3$] and with orange dashed line [$2 \leq A_1 < 3$], are included. Background layer surface geology (see Fig. 5).

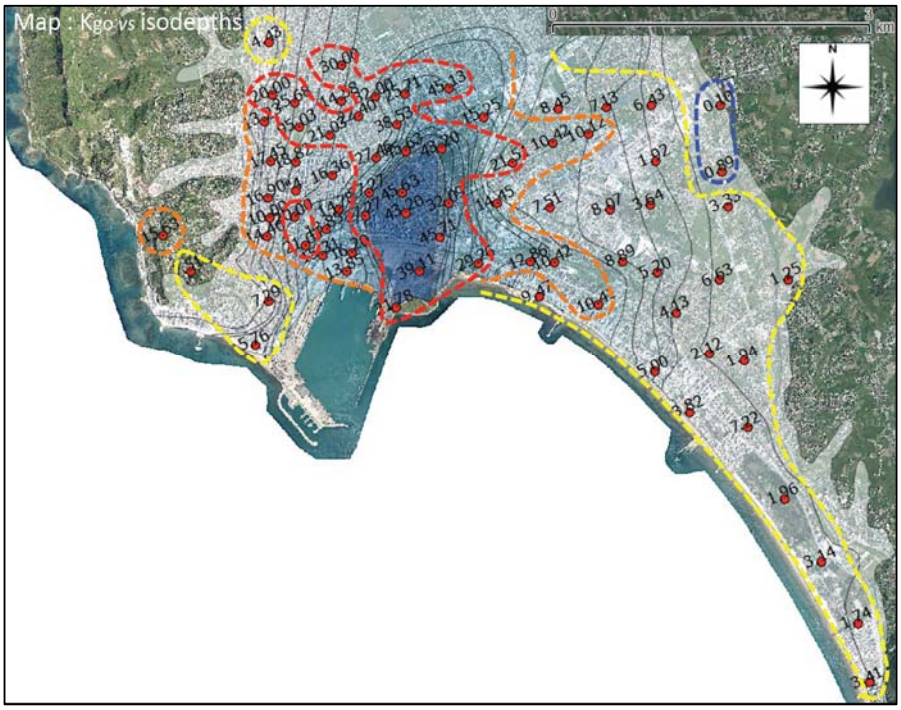

Fig. 22. Distribution of ground vulnerability index for fundamental frequency (Kgo) in the Durres city. For sites in areas with red dashed line [20≤Kgo≤95], with orange dashed line [10≤Kgo<20], with yellow dashed line [1≤Kgo<10] and with blue dashed line [Kgo<1], are included. Background layer isodepth contours per 10m (see Fig. 6).

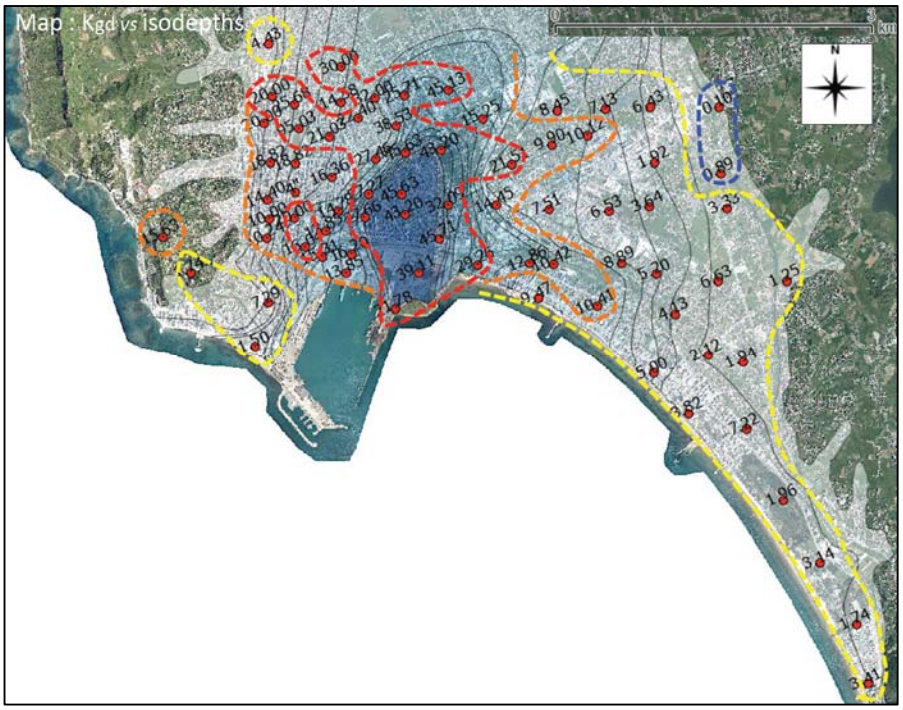

Fig. 23. Distribution of ground vulnerability index for dominant frequency (Kgd) in the Durres city. For sites in areas with red dashed line [20≤Kgd≤95], with orange dashed line [10≤Kgd<20], with yellow dashed line [1≤Kgd<10] and with blue dashed line [Kgd<1], are included. Background layer isodepth contours per 10m (see Fig. 6).

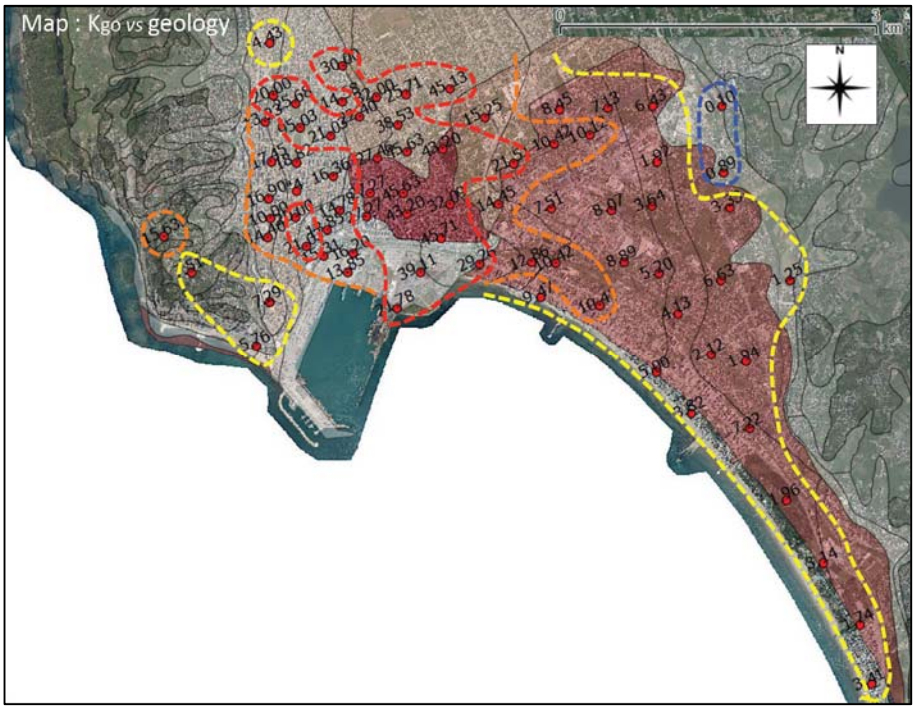

Fig. 24. Distribution of ground vulnerability index for fundamental frequency (Kgo) in the Durres city. For sites in areas with red dashed line [20≤Kgo≤95], with orange dashed line [10≤Kgo<20], with yellow dashed line [1≤Kgo<10] and with blue dashed line [Kgo<1], are included. Background layer surface geology (see Fig. 5).

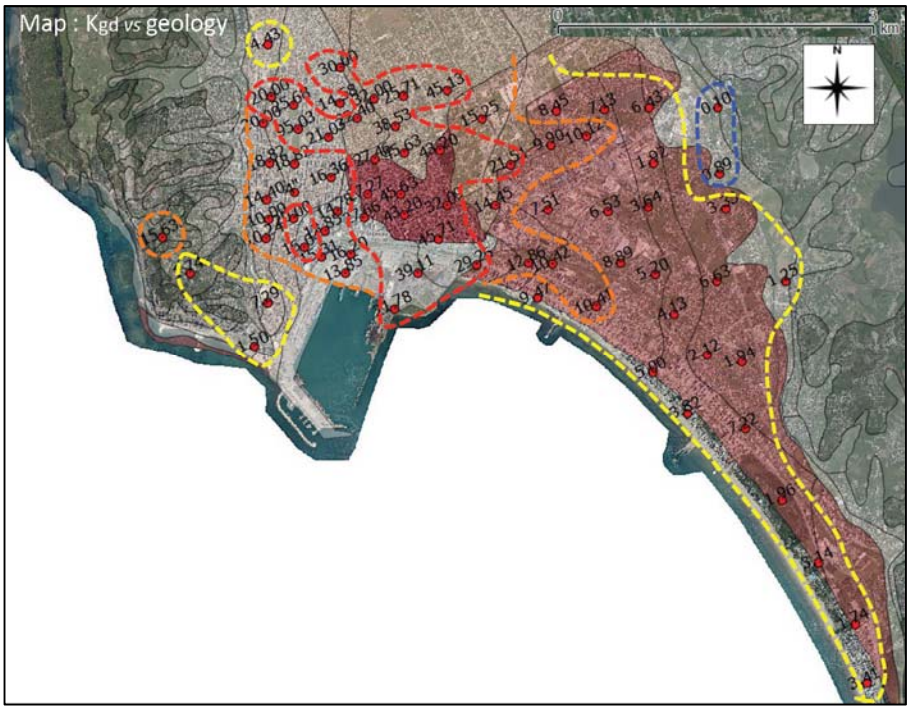

Fig. 25. Distribution of ground vulnerability index for dominant frequency (Kgd) in the Durres city. For sites in areas with red dashed line [20≤Kgd≤95], with orange dashed line [10≤Kgd<20], with yellow dashed line [1≤Kgd<10] and with blue dashed line [Kgd<1], are included. Background layer surface geology (see Fig. 5).

5. Discussion and Conclusions

In this work 76 single station ambient noise measurements were performed in the city of Durres within the period February 18 to 21, 2020, after the disastrous earthquake of Nov. 26, 2019 hit the city and cause heavy damage on built environment. The unique strong motion recording down-town the city (DURR accelerometric station) (Duni and Theodoulidis 2019) showed high spectral values in a wide range of periods ($0.2sec \leq T \leq 2.0sec$), implying existence of a low fundamental frequency ($fo \sim 0.5Hz$). From geologic and isodepth contours maps it is evident that the city is founded on a north-south trending basin of soft sediments reaching in its center around 130m depth. Surface geologic layers show low shear-wave velocity, with a $Vs_{30} \sim 200m/sec$.

Data processing and analyses based on Horizontal-to-Vertical (H/V) spectral ratio method showed that an extended part of the Durres city appeared a low fundamental frequency, $fo < 1.0Hz$. This part is mainly in the center-west side of the city, while fundamental frequency decreases towards the edge of the basin. The vast majority of examined sites (95%) exhibited amplitude of fundamental and dominant frequency greater than 2, reaching the value of ~6. Taking into account the scientific consensus that H/V peak amplitude represents a lowest threshold of actual ground amplification estimated by classical methods (e.g. Standard Spectral Ratio method), one would expect equal or/and higher amplification due to basin excitation by seismic wave-field. A second natural frequency peak, mainly in the western edge of the basin, may indicate either a thinner surface geologic layer of high contract interface with a deeper one or a more complex site response behavior due to edge basin geometry. Such an observation needs further theoretical 2D/3D modeling investigation.

A correlation between fundamental frequency and thickness of the soft sediments is observed, though with large dispersion due either to errors in depth estimation or to more superficial strata properties (e.g. soft colluvium, man-made deposits) not taken into account. Further geophysical and geotechnical investigation is needed to shed light in this issue.

The ground vulnerability index, Kg, though not widely accepted, showed that 62% of the investigated sites appeared values >10, related in some cases of other sites worldwide to damaged areas. Direct correlation of ground vulnerability index, Kg, values with respective damage level in the Durres city would provide valuable information for any seismic risk mitigation plan of the city.

Since earthquake damage interpretation is a multidisciplinary subject it undoubtedly requires respective scientific contribution from the civil engineering community as well as close collaboration between geoscientists and engineers in order to better understand earthquake effects on build environment.

Results of this work must be combined with additional geological, geophysical and geotechnical data as well as with theoretical 1D/2D/3D site response modeling to better understand site effects mechanism for the city of Durres. Any efficient seismic risk mitigation plan from future earthquake scenarios in the vicinity of the city, should definitely take into account such combined empirical and theoretical results and conclusions as well as close collaboration of geoscientists with engineers.

Acknewledgements

This work was financially supported by the IGEWE-PUT, Tirana and EBS sh.p.k. Company, Tirana. We greatly appreciate fruitful discussions with civil engineer Agim Seranaj on observed damage pattern in the Durres city that efficiently directed our experimental actions as well as our understanding of the complex nature of ground motion in the city.

References

Bard, P.-Y. (1999). "Microtremor Measurements: A tool for site effect estimation?", in the Effects of Surface Geology on Seismic Motion, (ed. Irikura, Kudo, Okada and Sasatani) Balkema, Rotterdam, 1251-1279.

Bard P-Y, SESAME Participants (2004) The SESAME project: an overview and main results, Proc. 13th WCEE, Paper No 2207.

Borcherdt (1970). Effects of Local Geology on Ground Motion near San Francisco Bay**,** Bull. Seismol. Soc. Am. 60, 29–61.

Duni, Ll. and Theodoulidis, N. (2019). Short note on the November 26, 2019, Durres (Albania) M6.4 earthquake: Strong ground motion with emphasis in Durres City. https://www.emsc-csem.org/Files/news/Earthquakes_reports/Short- Note_EMSC_31122019.pdf

Geopsy software (2020) [www.geopsy.org]

Haghshenas E, Bard PY, Theodulidis N (2008) Empirical evaluation of microtremor H/V spectral ratio. Bull. Earthq. Eng. 6(1):75–108

Koçiu S, Sulstarova E, Aliaj Sh, Duni Ll, Peçi V, Konomi N, Dakoli H, Fuga I, Goga K, Zeqo A, Kapllani L, Kozmaj S, Lika M. (1985). Seismic microzonation of Durresi town, internal report, (in Albanian), IGEWE, Tirane, Albania.

Konno, K., and Ohmachi T. "Ground-motion characteristics estimated from spectral ratio between horizontal and vertical components of microtremor", Bull. Seism. Soc. Am., 1998; 88:1, 228–241.

Lachet C. and Bard P-Y. (1994). Numerical and Theoretical Investigations on the Possibilities andLimitations of Nakamura's Technique, J. Phys. Earth. 42, 377–397.

Nakamura, Y. (1989). A method for dynamic characteristics estimation of subsurface using microtremor on the ground surface, QR Railway Tech. Res. Inst.,1989;30:25-33.

Nakamura Y. (2000). Clear identification of fundamental idea of Nakamura's technique and its applications, Proc. 12th WCEE,Paper No 2656.

Nogoshi, M. and Igarashi, T. (1971), On the Amplitude Characteristics of Microtremor (Part 2), J. Seism. Soc. Japan, 24: 26-40.

SESAME Guidelines (2004) [http://sesame.geopsy.org/SES_Reports.htm].

Theodoulidis N., Cultrera G., Tento A., Faeh D., Atakan K., Bard P-Y., Panou A., Haghshenas E., & the SESAME team (2004). Empirical evaluation of the Horizontal-to-Vertical spectral ratio technique: Results from the 'SESAME' prj., Proc. 13th WCEE, Paper No 2323.